

Reference details:

István Biró, Tibor Szalay (2016): “Extension of Empirical Specific Cutting Force Model for the Process of Fine Chip-removing Milling”, *Int J Adv Manuf Technol*, Vol. 84, Nb. 9-12, pp. 2735-2743, (DOI 10.1007/s00170-016-8957-x)

István Biró^{*1}, Tibor Szalay²

Extension of Empirical Specific Cutting Force Model for the Process of Fine Chip-removing Milling

^{1,2}Budapest University of Technology and Economics, Department of Manufacturing Science and Engineering, H-1111 Budapest, Műegyetem rkp. 3., Hungary

*Corresponding author: e-mail: biro@manuf.bme.hu, tel.: +3614632640, fax: +3614633176

Acknowledgements

The work reported in this paper is connected to the project “Talent care and cultivation in the scientific workshops of BME” project. The project is supported by grant TÁMOP-4.2.2.B-10/1--2010-0009. The authors would like to acknowledge the support provided by the CEEPUS III HR 0108 project. The current research is connected to the topic of the project TÉT-12_MX Hungarian-Mexican Bilateral Project “Experimental and theoretical optimization and control of machining technology and tool path for micro milling”. This research was partly supported by the EU H2020-WIDESPREAD-2014-1-FPA-664403 Teaming project “Centre of Excellence in Production Informatics and Control”. The authors would also like to express their gratitude to Sumitomo Electric Hardmetal Ltd. for making the milling tool and inserts available for the purpose of the current study.

Nomenclature:

f_z (mm) – feed rate per tooth

a_p (mm) – axial depth of cut

a_c (mm) – radial depth of cut

v_c (m/min) – cutting speed

m_n – total number of full rotations of the milling tool during force measurement

φ (rad) – angular position of the cutting edge during milling

ω (rad/s) – angular velocity of the cutting edge during milling

h (mm) – uncut chip thickness

b (mm) – uncut width of chip

A (mm²) – uncut chip section

h_b (μm) – boundary chip thickness

F (N) – cutting force

k (N/mm²) – specific cutting force

R^2 – standard coefficient for the determination of a regressed analytical curve with reference to the measured data

m_n – tool rotation index

M – total number of full tool rotations

s – corrected sample standard deviation (CSSD)

j – measuring coordinate system

j^* – local coordinate system of the cutting edge

$\underline{\mathbf{R}}$ – transformation matrix

Introduction and goals

Technological models are basic instruments of process planning and controlling methods in the field of general part manufacturing. In order to develop efficient technologies and to create accurate, precise predictions for ongoing procedures, up-to-date, multifunctional and exact numerical expressions are necessary. Besides accuracy, the term 'industrial efficiency' includes both time and cost saving aspects. This creates a demand for easy- and quickly-to-use, expressive mathematical models in the practical world of manufacturing.

Machining is still a leading technology in part shaping. Traditional mechanical cutting methods (e.g. turning, milling, drilling) are prevalent in feature-based geometry machining. [1, 2] However, processes and methods are required to be more increasingly precise due to stricter tolerance and higher quality demands concerning parts. [3] In fact, fine chip removal cutting processes are recognised as basic requirements for precision and micro part manufacturing. [4-8]

Cutting force components are major output parameters of mechanical cutting processes. They generally depend on the physical and chemical properties of the workpiece material, on the geometry of the cutting edge and on the applied technological parameters. The characteristics of the force components can be described by introducing a specific cutting force, as shown in Eq. (1).

$$k = F / A = F / (h \cdot b) \quad (1)$$

This definition is found in recent research of [1-5, 9-13]. However, in order to produce a more general, precise and flexible model of cutting forces, it is advisable to research and describe the cutting process at the levels of fundamental material deformation and surface contact mechanisms.

According to Wan et al. [14], three major mechanisms appear along the cutting edge: shearing and deformation of chip by the flank (primary cutting) edge, additional deformations by the bottom (secondary) edge, and rubbing / ploughing effects along the contacting surfaces. According to this view, the typical modelling aspects of the cutting force models can be summarized as follows [14]:

- a) Lumped mechanism models: only material deformation caused by the primary edge is relevant;
- b) Dual-mechanism models: deformation and rubbing / ploughing by the primary edge are taken into account;
- c) Triple-mechanism models: all presented mechanisms are concurrently reviewed.

Numerous researchers applied these models in their studies. In the analytical models of Merdol and Altintas [15] and others [3, 16-18], specific cutting force is defined as a parameter divided into two components: one component is caused by shear at the chip deformation zone and the other is related to rubbing between the tool and chip. Kaymakci et al. [19] integrated the effects of rubbing, tool geometry and the mechanical properties of edge coating on forces into a synthetical coefficient related to the actual cutting apparatus but also retained the classical aspect of specific cutting force.

The specific force coefficient (under specific conditions, a scalar force-type parameter of cutting) is often regarded as a standard linear coefficient in the case of a regressive model as it can be inspected in the examples mentioned above. However, there are classical approaches which focus on the physical manifestation of this special scalar. Specific cutting force can be approximated by exponential function based on uncut chip thickness, as presented in Eq. 2. This approach identifies specific cutting force coefficient as the cutting force needed to remove chips of a unit section. This interpretation follows the course of traditional cutting process modelling established by Taylor's famous 1907 expression of tool life [20]. Eq. 2 is still in use for industrial and research purposes due to its practicality and it directly appears in [1, 2, 10, 11, 21-25].

$$k = k_1 / h^m + \text{const.} \quad (2)$$

The characteristic of Eq. 2 well illustrates the size effect of cutting processes. According to Vollersten et al. [26] and indirectly mentioned by Fang et al. [27], in general part machining, three major types of size effects can be considered: the size effect of density, of shape and of microstructure. The classical model of Eq. 2 can be regarded as a mathematical approach of shape-type size effect due to its strict and obvious relation to uncut chip geometry.

However, there are more complex variations of modelling approaches of specific cutting force. Sambhav et al. [28] and others [29, 30] describe specific cutting force as a numerical, multi-componential, high-level (square and above) exponential function of workpiece material properties and machining parameters (feed rate, cutting speed). Other interpretations introduce the definition of instantaneous cutting force: Using their triple-mechanism model, Wan et al. [31, 32] and others [33, 34] defined special cutting force coefficients for every differential part of the cutting edge. This approach eliminates the standard definition of the specific force coefficient as an analytical parameter and in place of this it applies a model similar to finite element methods.

To conclude, specific cutting force is still a widely used parameter in the research, planning, simulation and controlling of mechanical cutting processes. The use of specific cutting force enables the creation of accurate, standardisable models for cutting operations using defined materials and tools with reference to a wide range of technological parameters. However, according to the studies reviewed, these specific force based models fail to represent specific cutting force as an indicator of the quality of material deforming processes. Specific cutting force is interpreted as a cutting-parameter, which, on the one hand, depends on the results of the relevant coefficients and the application of which, on the other hand, results in elaborate mathematical models. However, these studies give a less definite answer about the tendencies of cutting forces during processes exhibiting complex kinematics such as milling. The aim of the current research is to resolve this problem in the form of offering a practically applicable yet precise and up-to-date model of machining focusing on changes in geometrical and kinematical conditions during chip-removing.

1. Boundary chip thicknesses in the logarithmic model of specific cutting forces

A classical adaptation of the definitions of specific cutting force and coefficient is the Kienzle-Victor model [35] of 1957. It is formulated as a multi-parameterised, chip-geometry based exponential expression presented in Eq. 3 and its logarithmic linearised form appears in Eq. 4.

$$F = k_1 \cdot b \cdot h^{(1-m)} \quad (3)$$

$$\lg F = \lg k_1 + \lg b + (1 - m) \cdot \lg h \quad (4)$$

This model has been designed in a way that it is adaptable to any mechanical cutting operations using a wide range of cutting parameters yet it is easy-to-handle and telling of force tendencies. However, the original Kienzle-expression was developed for macro-machining and its validity for the scale of micro-chip removal is highly questionable because of the intense presence of size effect. Classical studies, such as Bali [36], described specific cutting force as a multi-partitioned function through defining boundary values of uncut chip thickness (h_b) but did not mention the exact tendencies on the level of micro-chip. Brandão de Oliveira et al. [13] investigated the validity of Kienzle's model for micro-milling. They revealed some differences in the classical model coefficients of k_1 and m . These differences may be caused by the different material deforming mechanisms occurring at different chip thicknesses. Based on this theory, the stages of chip removing process were ranked in our previous research [37] as follows:

- Zone I: cutting using macro chip geometry with boundaries $h \geq 0.1$ mm;
- Zone II: cutting using fine chip geometry with boundaries $0.01 \leq h < 0.1$ mm;
- Zone III: cutting by removing micro-scale chip with boundaries $0.003 \leq h < 0.01$ mm;
- Zone IV (hypothetical): micro-chip removal with an increased effect rate due to ploughing and rubbing compared to shearing mechanisms of uncut chip thickness of $h < 0.003$ mm.

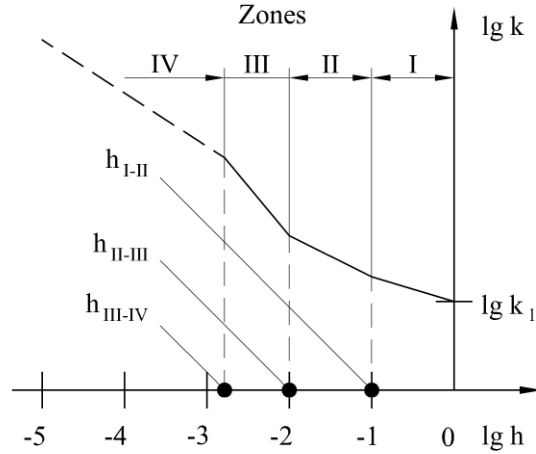


Fig. 1 Multi-partitioned specific cutting force model in the logarithmic system [32]

The supposed existence and characteristics of Zone IV (as presented in Figure 1) were based on data of our previous partial factorial experiment. The results of FEM-simulation performed by Altintas and Jin [5] indicate the same theory. Experimental data of Ko et al. [11] and others [10, 12, 21, 38, 39] also suggest this. Brandão de Oliveira et al. [13] partitioned the chip-removing process into sections for micro-milling according to suspected deformation mechanisms based on chip observations. However, they did not consider the possible application of a partitioned force model on the level of fine- and micro-chip.

As mentioned before, the model of Eq. 3 is based on the geometry of the uncut chip section. The accuracy of this expression is highly dependent on the geometrical model of cutting. Due to the kinematics of milling, cutting edge follows a trochoidal path. There are precise approximations for chip thickness, e.g. coordinate-geometrical and numerical models by Tukora and Szalay [16], Rao et al. [40] and others [41-44]. However, for practical modelling purposes a simplified basic model of chip thickness (see Eq. 4 and Figure 1) can be adequately precise as it is demonstrated by Gonzalo et al. [18] and others [1, 2, 12, 21]. The model presented in Figure 1 is based on the geometrical approach of Eq. 4.

$$h = f_z \cdot \sin \varphi \quad (4)$$

Our previous studies [37, 45] support the idea of a multi-partitioned force model for cutting operations using instantaneous chip geometry. However, the lack of enough data and parameter settings necessitated a new, more precise and extended experiment with a well-established evaluation method. The specific aim of the current research is both to validate the multi-partitioned model of specific cutting force for the circumstances of fine-milling and to describe the effect of the cutting parameters on the sections of the force model in the form of a simple but practical, yet statistically accurate and expressive model.

2. Face milling experiments

Our previous studies were based on partial factorial design. The results of these experiments strongly implied the validity of the force-characteristics presented in Figure 1. In order to get a mathematically and statistically accurate model, the experiments of the current research were based on a full factorial design with an extended range of parameters. Due to the logarithmic evaluation method, the classical Kienzle parameters (feed rate, depth of cut) were set by geometric progression in order to create a representative measurement data field. Cutting speed followed an arithmetic progression due to the limited domain of realisable parameter configurations. A total number of 90 experiments were carried out with different parameter settings, as shown in Table 1.

Factors	Cutting speed	Feed rate	Depth of cut	Width of cut	Direction of cut
	v_c (m/min)	f_z (mm/tooth)	a_p (mm)	a_e (mm)	DIR (-)
Levels	50; 75; 100; 125; 150	0.01; 0.04; 0.16	0.5; 1.0; 2.0	8	climb; conventional

Table 1. Factors of face milling experiments

Face milling experiments were completed on a Kondia B640 3-axis CNC milling machine using Sumitomo AXMT123504PEERG milling inserts in a Sumitomo WEX2016E tool holder. The tool was used as a single-pointed cutter. The material of the workpiece was S960QL high strength structural steel ($R_{p0.2} = 960$ MPa, $R_{eH} = 980 \dots 1150$ MPa, HRC = 36, C% = 0.2; Si% = 0.8; Mn% = 1.7; Cr% = 1.5; Ni% = 2.0; Mo% = 0.7; V% = 1.2). Force measurement was realized by a 3-component Kistler 9257A piezoelectric sensor and a Kistler 5019 charge amplifier. An Omron E3F-DS10B4 reflective optical sensor provided the reference signal of the angular position of the cutting edge. Semi-automatic data acquisition was carried out applying a National Instruments USB-4431 unit connected to a LabView measuring software specially developed for the purposes of the current research. The wearing condition of the tool was checked via Dinoware AM431ZT and Dinoware AM413TL digital microscopes. All equipment used are the property of the Department of Manufacturing Science and Engineering. The kinematics of performed face millings is presented in Figure 2.

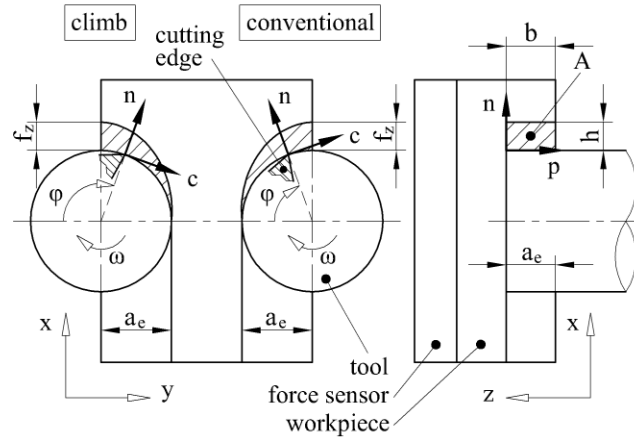


Fig. 2 The kinematics and coordinate systems of cutting

3. Representation of specific cutting forces

3.1 Modelling system

In the scope of this research, the modelling approach of specific cutting forces is identical to the classical interpretation of Eq. (1-2). The commonly used sinusoidal approximation of uncut chip thickness in Eq. (2) is accurate enough to represent the results in the current stage of our research: as the presumed new tendencies are statistically indefinite, the first step of modelling method includes only the basic, scientifically and practical approved analytical expressions. For this, two coordinate systems need to be defined in line with Figure 2:

- $j = [x,y,z]$: local system defined by the standard coordinates of the piezoelectric sensor;
- $j^* = [c,n,p]$: local system attached to the cutting edge.

With this in mind, specific cutting forces can be described as:

$$k_{j^*} = F_{j^*} / (h \cdot b) = F_{j^*} / (f_z \cdot \sin \phi \cdot a_p) \quad (5)$$

As seen in Eq. (5), cutting forces are defined in the local coordinate system of the cutting edge. Therefore, a transformation of measured forces is required, for which the application of an **R** transformation (rotating) matrix is used, as shown in Figure 2:

$$[\underline{\mathbf{F}}(\varphi)]_{j^*} = \underline{\mathbf{R}}(\varphi) \cdot [\underline{\mathbf{F}}(\varphi)]_j \quad (6)$$

The **R** transformation matrix can be expressed as an expression of measured independent variables and machining parameters based on Eq. (1,5,6) and Figure 3, and considering that $\varphi = \omega \cdot t$:

$$[k(\omega t)]_{j^*} = \frac{1}{f_z \cdot a_p} \cdot \frac{\underline{\mathbf{R}}(\omega t) \cdot [\underline{\mathbf{F}}(\omega t)]_j}{\sin(\omega t)} \quad (7)$$

where $t_0 \leq t \leq t_{\text{meas}}$ is the time interval of measurement and t_0 is adjusted to the reference angular position (see φ_0 in Figure 2).

3.2 Measurement statistics

Data of measured force during cutting experiments, especially during milling processes, generally have high deviations around the mean value due to the intensive dynamic actions involved. In order to create reliable models, statistical examination of data is required.

Milling forces have periodic tendencies, where periodicity is defined by the angular velocity of the cutting tool. Therefore, the theoretical mean values of cutting forces are repeated m_n times during measurement, where m_n is the index-number of current tool rotation and M is the total number of measured rotations. The data acquisition method of milling forces can be regarded as a measuring sequence of forces in the same angular position of the cutting edge as above, while the measuring series of forces is defined by the periodically repeated angular position of the cutting edge as presented in Eq. (8). Therefore, mean characteristics (discrete functions of mean values as per angular position) of milling forces can be calculated according to Eq. (9).

$$(m_n - 1) \cdot 2\pi \leq (\varphi = \omega t) < m_n \cdot 2\pi \quad m_n = 1, 2, 3, \dots, M \quad (8)$$

$$\bar{F}(\omega t) = \sum_{m_n=1}^M \frac{F_{m_n}(\omega t)}{M} \quad (9)$$

With reference to Eq. (8-9) and of the indexes of the specified coordinate systems, the corrected sample standard deviation (CSSD) of measured force data can be calculated according to Eq. (10):

$$(s_{F_j}(\omega t))^2 = 1/(M-1) \cdot \sum_{m_n=1}^M (F_{m_n,j}(\omega t) - \bar{F}_j(\omega t))^2 \quad (10)$$

4. Results and discussion

According to the classification of Wan et al. [14] (introduced in Section 1), the current cutting force based representation of the milling process can be regarded as a triple-mechanism model. Even so, due to the applied experimental and modelling methods, it neglects the characterization of the individual mechanisms occurring at the cutting edge. In fact, our current research was clearly focused on the general effect of the cutting parameters on cutting forces: the aim was to refine the model of

specific cutting force. With a view to this, a new section of characteristics was defined in order to extend the validity of the classical model to cutting using micro-chip thickness.

4.1 Definition of new boundary chip thickness

Semi-automatic data evaluation and model fitting were carried out by a software application developed for the purposes of the current research in LabView 2013. Low-pass filtering at 1000 Hz was applied to decrease the noise-effect of vibrations in the measured data of force without any distortion to the main characteristics. Mean value calculations, statistics and the modelling structure strongly implied the existence of a new boundary chip thickness (h_b) in the case of micro-chip removal, thus the results are in correlation with our previous studies. Furthermore, the new boundary chip thickness fits strikingly into the geometric progression of other known boundary values, as it is shown in Figures 3 and 4 (these two figures use the same indexes as Figure 1 above).

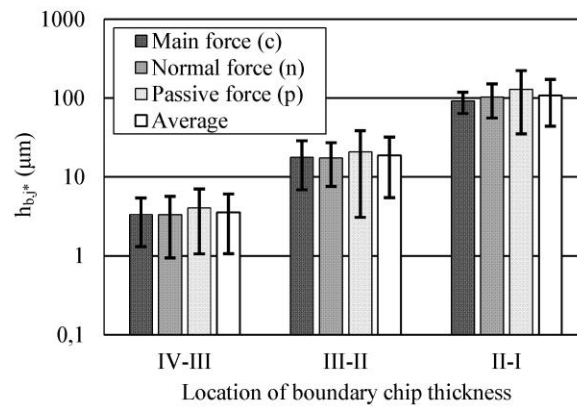


Fig. 3 Measured boundary chip thickness with standard deviation broken down by cutting force components

Linear regression in the logarithmic system proved to be the most accurate analytical approximation of measured data as per the variance of regression. The general interpretation of the regressive curve is:

$$\lg h_{b,i,j^*} = C_h + x_h \cdot i \quad (11)$$

where i is the index to identify the boundaries of intercepting specific force sections (as shown in Table 2). Through the transformation of Eq. (11) to the metric system, a general empirical model of boundary chip thickness can be established:

$$h_{b,i,j^*} = C_{h1,j^*} \cdot C_{h2,j^*}^i \quad (\mu\text{m}) \quad (12)$$

and $C_{h1,j^*} = 10^{C_{h,j^*}}$, $C_{h2,j^*} = 10^{x_{h,j^*}}$

where i is the index of boundary chip thickness and j^* is the index of the cutting force component. The coefficients of Eq. (11-12) are summarized in Table 2. Measured and calculated results are presented in Table 3. The new boundary chip thickness is defined with reference to the value of uncut chip thickness $h = 3 \dots 4 \mu\text{m}$. Figure 4 shows the regression method concerning the measured data and the measurement's standard deviation. The new boundary chip thickness easily fits into to existing model of boundary chip thicknesses.

It is noteworthy that Brandão de Oliveira et al. [13] referred to a feed rate of $f_z = 3 \mu\text{m/tooth}$ to be the technological boundary of macro- and micro-scale machining. They correlate this value to the method of minimum size chip removal, which is highly dependent on the properties of the workpiece material and cutting edge geometry. For further implications, see Section 5.3.

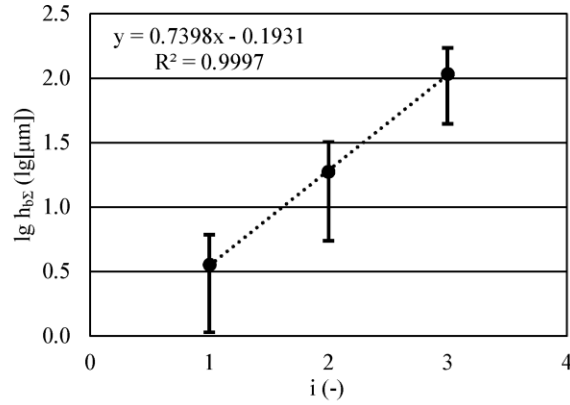


Fig. 4 Regression method applied to the average values of boundary chip thickness

j^*	C_h	x_h	R^2	C_{h1}	C_{h2}
Main force (c)	-0.1884	0.7174	1.0000	0.6480	5.2167
Normal force (n)	-0.2338	0.7464	0.9995	0.5837	5.5770
Passive force (p)	-0.1567	0.7517	0.9991	0.6971	5.6454
Average (Σ)	-0.1931	0.7398	0.9997	0.6411	5.4929

Table 2. The coefficients of linear regression on boundary chip thickness values in the logarithmic system

Intercepting sections		$h_{b,i,meas}$ (μm)				$h_{b,i,cal}$ (μm)	
Boundary	i	Main	Normal	Passive	Average	Average	Relative error of averages
IV-III	1	3.4	3.3	4.1	3.6	3.5	- 2.8%
III-II	2	17.8	17.4	20.9	18.7	19.3	3.2%
II-I	3	91.5	103.5	129.2	108.1	106.3	- 1.7%

Table 3. The application of new boundary chip thickness in the system of known boundaries of specific cutting forces

Figure 5 presents a calculated result based on the model in Eq. (11) and the coefficients in Table 2. CSSD of measured data with reference to the model mean values was also defined using Eq. (10). Figure 5 clearly shows that, based on the deviation with reference to the model means, the new boundary chip thickness must exist beside the already known boundaries of specific cutting forces.

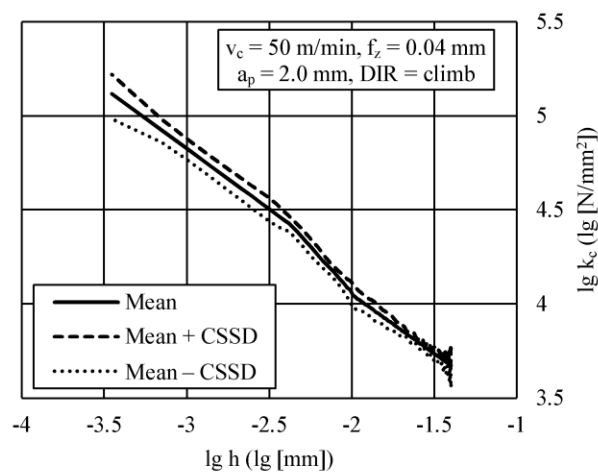


Fig. 5 Modelling the main specific cutting force

4.2 The effect of cutting parameters on new boundary chip thickness

ANOVA of measured data indicates that feed rate has the greatest impact on the value of boundary chip thickness. Strictly speaking, the effects of depth of cut, cutting speed and direction of cut are impossible to define based on current measurement data. From the aspect of modelling accuracy, these parameters seem to have a negligible impact on the position of boundary chip thickness (excluding feed rate). This may be closely related to the fact that differences of h_b mean values are below measurement accuracy.

However, it is possible that the effect of feed rate can be modelled with the help of a single surface regression thereby creating an indirect indicator to validate the existence of the newly defined boundary chip thickness. Figure 6 indicates that a rising feed rate causes boundary chip thicknesses to also increase. Linear surface regression on the logarithmic data revealed that it is possible to create a model based on the parameter of feed rate as described in Eq. (13) and shown in Figure 7. But this is still hypothetical because of the insufficient number of feed rate levels. With reference to this, the coefficients of Eq. (13) are summarized in Table 3.

$$\lg h_{b,i,j^*} = C_h' + x_h' \cdot i + y_{h,j} \cdot \lg f_z \quad (13)$$

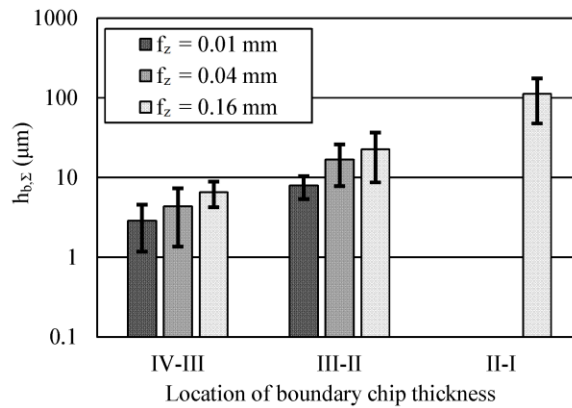


Fig. 6 Measured boundary chip thicknesses with standard deviation as per feed rate

j^*	C_h'	x_h'	y_h	R^2
Average (Σ)	0.5891	0.5218	0.3384	0.9968

Table 3. Coefficients of the linear surface regression on boundary chip thickness values in the logarithmic system

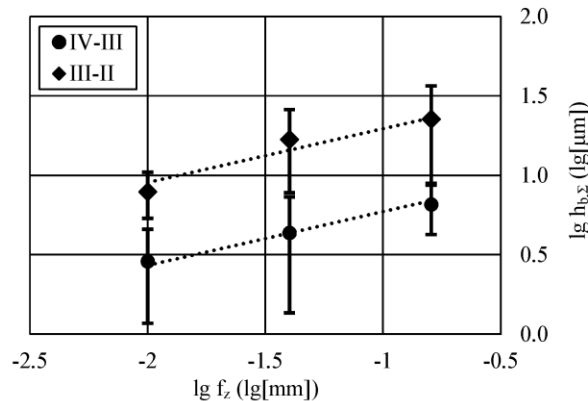


Fig. 7 The representation of the surface regression model on average values of boundary chip thickness

4.3 Tool geometry and workpiece material

Tool geometry and tool wear were not in the focus of the current research. Therefore, tool wear was controlled by checking the extension of the wearing mechanism. A limit of 0.1 mm flank wear was defined as maximum admissible wear on both the primary and secondary edges. The executing order of experimental parameter setting was optimised for the minimization of the observable effect of tool wear on cutting forces. The nominal geometry of the cutting edge was not altered, therefore the effect of cutting angles and edge radii is not definable. Even so, edge radii have a primary impact on minimum chip thickness (see e.g. [13]). This issue will be under scrutiny in further studies involving micro-machining.

The magnitude of forces to realize breakage (therefore creating chip) is primarily related to the hardness of material while stiffness and persistence define the quality of elastic and plastic deformations prior to actual chip formation. S960QL is regarded to have modest hardness but its persistence is higher than that of more commonly used structural steels (e.g. S235J2+N). More persistent materials tend to produce traits of cutting force, which are good indicators of the different deforming processes in chip formation. Thus, the characteristics of new boundary chip thickness are easier to observe. Further research will extend to the cutting of materials with different chemical, structural and mechanical properties: C45 carbon steel will be examined due to its high persistence and very low hardness, and hard-cutting experiments will also be realized to measure the effect of extreme but controlled hardness. The currently used S960QL shall be used as base material due to its overall high-middle-class properties and because its cutting forces reliably indicate the quality of new boundary chip thickness.

5. Conclusions

Experimental and statistical results of the current research indicate that extension of classic specific cutting force model is possible by defining a new boundary section of uncut chip thickness with great precision according experimental force data. Therefore, a new boundary chip thickness exists in the case of micro-chip formation. This is observable with reference to uncut chip thickness of $h = 3 \dots 4 \mu\text{m}$ during the face milling of S960QL high strength structural steel. The new parameter can be modelled by a linear function in the logarithmic system along with the other known section boundaries. Thus, the new boundary neatly fits into the classical model of multi-sectioned specific cutting force. The existence of the boundary is hypothetically proved by the suspected change in the quality of material deforming processes.

The mean value of the new boundary chip thickness mostly depends on feed rate. Furthermore, a linear correlation is suspected between the feed rate and the value of boundary chip thickness in the logarithmic system. Other boundaries show similar behaviours but this has not yet been proved due to the insufficient number and scale of parameters in the scope of the experiments of the current research. The effect of other cutting parameters – i.e. that of depth of cut, cutting speed and direction of cut – is not definable analytically based on the current data. Further experiments as well as an extended number and scale of parameters and data are required for further research. Also, specific experiments are necessary for validating the model regarding the effect of feed rate. Likewise, future research in this field will extend to the examination of chip formation and deforming processes in different materials by way of the application of cutting experiments and finite element simulations. Another aim of future research is to validate and apply the extended model to cutting parts using different (micro-) cutting technologies (e.g. turning).

References

- [1] Anand RS, Patra K, Steiner M (2014) Size effects in micro drilling of carbon fiber reinforced plastic composite. *Production Engineering - Research and Development*, 8(3):301-307. doi: 10.1007/s11740-014-0526-2

- [2] Andersson C, Andersson M, Ståhl JE (2011) Experimental studies of cutting force variation in face milling. *Int J Mach Tool Manu* 51(1):67-76. doi: 10.1016/j.ijmachtools.2010.09.004
- [3] Wojciechowski S (2015) The estimation of cutting forces and specific force coefficients during finishing ball end milling of inclined surfaces. *Int J Mach Tool Manu* 89:110-123. doi: 10.1016/j.ijmachtools.2014.10.006
- [4] Altintas Y, Jin X (2011) Mechanics of micro-milling with round edge tools. *CIRP Ann-Manuf Techn* 60(1):77-80. doi: 10.1016/j.cirp.2011.03.084
- [5] Jin X, Altintas Y (2012) Prediction of micro-milling forces with finite element method. *J Mater Process Tech* 212(3):542-552. doi: 10.1016/j.jmatprotec.2011.05.020
- [6] Takács M, Verő B, Mészáros I (2003) Micromilling of metallic materials. *J Mater Process Tech* 138(1–3):152-155. doi: 10.1016/S0924-0136(03)00064-5
- [7] Takács M, Verő B (2003) Material Structural Aspects of Micro-Scale Chip Removal. *Material Science Forum*, 414–415:377-342. doi: 10.4028/www.scientific.net/MSF.414-415.337
- [8] Mészáros I, Farkas BZs, Keszenheimer A (2010) New cutting edge geometries for high precision hard turning. *Proceedings of 4th CIRP International Conference on High Performance Cutting* 2:351-356. ISBN: 978-4-915698-03-3
- [9] Altintas Y, Kersting P, Biermann D, Budak E, Denkena B, Lazoglu I (2014) Virtual process systems for part machining operations. *CIRP Ann-Manuf Techn* 63(2):585-605. doi: 10.1016/j.cirp.2014.05.007
- [10] Campatelli G, Scippa A (2012) Prediction of Milling Cutting Force Coefficients for Aluminum 6082-T4. *Procedia CIRP* 1:563-568. doi: 10.1016/j.procir.2012.04.100
- [11] Ko JH, Yun WS, Cho DW, Ehmann KF (2002) Development of a virtual machining system, part 1: approximation of the size effect for cutting force prediction. *Int J Mach Tool Manu* 42(15):1595-1605. doi: 10.1016/S0890-6955(02)00137-2
- [12] Srinivasa YV, Shunmugam MS (2013) Mechanistic model for prediction of cutting forces in micro end-milling and experimental comparison. *Int J Mach Tool Manu* 67:18-27. doi: 10.1016/j.ijmachtools.2012.12.004
- [13] de Oliveira FB, Rodrigues AR, Coelho RT, de Souza AF (2015) Size effect and minimum chip thickness in micromilling. *Int J Mach Tool Manu* 89:39-54. doi: 10.1016/j.ijmachtools.2014.11.001
- [14] Wan M, Lu MS, Zhang WH, Yang Y (2012) A new ternary-mechanism model for the prediction of cutting forces in flat end milling. *Int J Mach Tool Manu* 57:34-45. doi: 10.1016/j.ijmachtools.2012.02.003
- [15] Merdol SD, Altintas Y (2008) Virtual cutting and optimization of three-axis milling processes. *Int J Mach Tool Manu* 48(10):1063-1071. doi: 10.1016/j.ijmachtools.2008.03.004
- [16] Tukora B, Szalay T (2011) Real-time determination of cutting force coefficients without cutting geometry restriction. *Int J Mach Tool Manu* 51(12):871-879. doi: 10.1016/j.ijmachtools.2011.08.003
- [17] Denkena B, Vehmeyer J, Niederwestberg D, Maaß P (2014) Identification of the specific cutting force for geometrically defined cutting edges and varying cutting conditions. *Int J Mach Tool Manu* 82-83:42-49. doi: 10.1016/j.ijmachtools.2014.03.009
- [18] Gonzalo O, Beristain J, Jauregi H, Sanz C (2010) A method for the identification of the specific force coefficients for mechanistic milling simulation. *Int J Mach Tool Manu* 50(9):765-774. doi: 10.1016/j.ijmachtools.2010.05.009
- [19] Kaymakci M, Kilic ZM, Altintas Y (2012) Unified cutting force model for turning, boring, drilling and milling operations. *Int J Mach Tool Manu* 54-55:34-45. doi: 10.1016/j.ijmachtools.2011.12.008
- [20] Szalay T (2009) Modelling in Metal Cutting Theory. In: Barišić B (ed) *Concurrent Product and Technology Development, Fintrade and Tours, Kastav*, pp 85-102. ISBN: 978-953-96899-9-3

- [21] Balogun VA, Mativenga PT (2014) Impact of un-deformed chip thickness on specific energy in mechanical machining processes. *J Clean Prod* 69:260-268. doi: 10.1016/j.jclepro.2014.01.036
- [22] Wan M, Zhang WH, Dang JW, Yang Y (2010) A novel cutting force modelling method for cylindrical end mill. *Appl Math Model* 34(3):823-836. doi: 10.1016/j.apm.2009.09.012
- [23] Ahn IH, Moon SK, Hwang J (2015) A mechanistic cutting force model with consideration of the intrinsic and geometric size effects decoupled. *Int J Adv Manuf Tech* 81:745-753. doi: 10.1007/s00170-015-7227-7
- [24] Zhang T, Liu Z, Xu C (2015) Theoretical modeling and experimental validation of specific cutting force for micro and milling. *Int J Adv Manuf Tech* 77:1433-1441. doi: 10.1007/s00170-014-6549-1
- [25] Perez H, Diez E, Marquez JJ, Vizan A (2013) An enhanced method for cutting force estimation in peripheral milling. *Int J Adv Manuf Tech* 69:1731-1741. doi: 10.1007/s00170-013-5153-0
- [26] Vollertsen F, Biermann D, Hansen HN, Jawahir IS, Kuzman K (2009) Size effects in manufacturing of metallic components. *CIRP Ann-Manuf Techn* 58(2):566-587. doi: 10.1016/j.cirp.2009.09.002
- [27] Fang F, Xu F, Lai M (2015) Size effect in material removal by cutting at nano scale. *Int J Adv Manuf Tech* 80:591-598. doi: 10.1007/s00170-015-7032-3
- [28] Sambhav K, Kumar A, Choudhury SK (2011) Mechanistic force modeling of single point cutting tool in terms of grinding angles. *Int J Mach Tool Manu* 51(10-11):775-786. doi: 10.1016/j.ijmachtools.2011.06.007
- [29] Subramanian M, Sakthivel M, Sooryaprakash K, Sudhakaran R (2013) Optimization of end mill tool geometry parameters for Al7075-T6 machining operations based on vibration amplitude by response surface methodology. *Measurement* 46 (10):4005-4022. doi: 10.1016/j.proeng.2013.09.144
- [30] Salguero J, Batista M, Calamaz M, Girot F, Marcos M (2013) Cutting Forces Parametric Model for the Dry High Speed Contour Milling of Aerospace Aluminium Alloys. *Procedia Engineering* 63:735-742. doi: 10.1016/j.proeng.2013.08.215
- [31] Wan M, Zhang WH, Qin GH, Tan G (2007) Efficient calibration of instantaneous cutting force coefficients and runout parameters for general end mills. *Int J Mach Tool Manu* 47(11):1767-1776. doi: 10.1016/j.ijmachtools.2006.06.012
- [32] Wan M, Pan WJ, Zhang WH, Ma YC, Yang Y (2014) A unified instantaneous cutting force model for flat end mills with variable geometries. *J Mater Process Tech* 214(3):641-650. doi: 10.1016/j.jmatprotec.2013.10.016
- [33] Wang M, Gao L, Zheng Y (2014) An examination of the fundamental mechanics of cutting force coefficients. *Int J Mach Tool Manu* 78:1-7. doi: 10.1016/j.ijmachtools.2013.10.008
- [34] Kao YC, Nguyen NT, Chen MS, Su ST (2015) A prediction method of cutting force coefficients with helix angle of flat-end cutter and its application in a virtual three-axis milling simulation system. *Int J Adv Manuf Tech* 77:1793-1809. doi: 10.1007/s00170-014-6550-8
- [35] Kienzle O, Victor H (1957) Spezifische Schnittkräfte bei der Metallbearbeitung. *Werkstattstechnik und Maschinenbau* 47:22-25.
- [36] Bali J (1985) *Forgácsolás*. (in Hungarian) Tankönyvkiadó, Budapest. ISBN: 963-18-0806-8
- [37] Biró I, Czampa M, Szalay T (2015) Experimental model for the main cutting force in face milling of a high strength structural steel. *Period Polytech Mech* 59(1):8-15. doi: 10.3311/PPme.7516
- [38] Liu K, Melkote SN (2005) Material Strengthening Mechanisms and Their Contribution to Size Effect in Micro-Cutting. *J Manuf Sci E-T ASME* 128(3):730-738. doi: 10.1115/1.2193548
- [39] Afazov SM, Ratchev SM, Segal J, Popov AA (2012) Chatter modelling in micro-milling by considering process nonlinearities. *Int J Mach Tool Manu* 56:28-38. doi: 10.1016/j.jmatprotec.2012.12.001

- [40] Rao VS, Rao PWM (2005) Modelling of tooth trajectory and process geometry in peripheral milling of curved surfaces. *Int J Mach Tool Manu* 45(6):617–630. doi: 10.1016/j.ijmachtools.2004.10.004
- [41] Kumanchik LM, Schmitz TL (2007) Improved analytical chip thickness model for milling. *Precision Engineering* 31(3):317-324. doi: 10.1016/j.precisioneng.2006.12.001
- [42] Kang YH, Zheng CM (2013) Mathematical modelling of chip thickness in micro-end- milling: A Fourier modelling. *Appl Math Model* 37(6):4208-4223. doi: 10.1016/j.apm.2012.09.011
- [43] Sun Y, Guo Q (2011) Numerical simulation and prediction of cutting forces in five-axis milling processes with cutter run-out. *Int J Mach Tool Manu* 51(10-11):806-815. doi: 10.1016/j.ijmachtools.2011.07.003
- [44] Takács M, Verő B(2007) Actual Feed Rate per Tooth at Micro Milling. *Material Science Forum* 537-538:695-700. doi: 10.4028/www.scientific.net/MSF.537-538.695
- [45] Biró I, Szalay T, Markos S (2013) Machinability of S960QL high strength structural steel: energetic description of cutting at small chip-thickness in face milling. *International Conference on Innovative Technologies (IN-TECH 2013)* 237-240. ISBN: 978-953-6326-88-4